

Thermodynamic Equilibrium of Water and Ice in Hydrated Gliadin and Hemoglobin

G. Sartor and G. P. Johari*

Department of Materials Science and Engineering, McMaster University, Hamilton, Ontario L8S 4L7, Canada

Received: March 12, 1997; In Final Form: May 28, 1997[⊗]

Crystallization of water and the water–ice equilibrium in the hydrated states (1 g of H₂O/g of dry protein) of gliadin and hemoglobin have been studied by differential scanning calorimetry. Water and ice coexist at a thermodynamic equilibrium at all temperatures in the 230–272 K range. Their relative amounts have been determined from 260 to 273 K, and a formalism based on equilibrium thermodynamics has been developed. The temperature dependence of the equilibrium constant of the water ↔ ice interconversion does not obey the Gibbs–Helmholtz equation, and this indicates a strong interaction of proteins with water. By using the measured equilibrium constant at different temperatures and the difference between the C_p of the solutions in equilibrium with ice and the ice itself in the hydrated proteins, the DSC scans obtained during cooling have been simulated. The kinetics of crystallization is not determined entirely by the grain-growth process. A double crystallization peak has been observed on cooling hydrated gliadin from 274 K, after the sample had been thermally cycled in the 230–273 K range and annealed at 274 K. Among the nine contributions to the enthalpy and entropy change on cooling and annealing at subfreezing temperatures, the largest contribution remains that from water's crystallization in the hydrated proteins. The amount of water in equilibrium with ice in the two proteins is comparable to that determined for relatively impure proteins. This underscores the importance of H-bond interaction with the protein molecules over that of the effects of impurities.

Introduction

That proteins absorb water has been common knowledge for many decades, but the specific role of water in protein dynamics that makes native proteins biologically active has been recognized only recently.^{1–3} To understand this role, several techniques have been used to investigate the physical and chemical processes that occur in proteins in the presence of varying amounts of water.^{1–6} As a result of these studies, it is now known that some of this water acts by hydrogen bonding to the amino, carboxyl, and hydroxyl groups in a protein's macromolecule and the rest by increasing the conformational and configurational changes in a protein's structure: the latter makes it plastically deformable. Mayer and co-workers^{4–9} have done detailed calorimetric studies of relatively pure, hydrated proteins which provide information on how interaction with water increases the conformational and configurational degrees of freedom and the rates of localized diffusion of segments and groups in protein molecules, e.g., myoglobin,⁵ hemoglobin,⁵ and lysozyme,⁵ and the DNA's polynucleotide or nucleic acid structures^{7,8} at low temperatures. They further showed that segregation or clustering of water molecules in a hydrated protein's structure occurs on annealing before the water freezes to ice in the 260–273 K region.¹⁰ A corresponding study of structurally inhomogeneous mixtures of food proteins,^{11–14} such as beef¹¹ and hydrated gluten¹² and soybean,¹⁴ containing organic molecules, lipids, carbohydrates, and inorganic salts and ions, led Sartor and Johari to conclude that the thermokinetic manifestations of distribution of configurational and conformational energy barriers to molecular or segmental motions in proteins are remarkably similar to those observed in studies on hydrated poly(2-hydroxyethyl methacrylate)¹⁵ and cross-linked interpenetrating network polymers, some of which, such as 25% poly(urethane)–75% poly(methyl methacrylate), do not absorb significant amounts of water.¹⁶

These studies led to investigations into the manner in which water in a hydrated protein crystallizes during both (i) heating

its vitrified state and (ii) annealing of its ice-containing state at high temperatures. These showed that a thermodynamic equilibrium between ice and water (or a freeze-concentrated aqueous solution) is maintained in complex mixtures of food proteins^{11,12,14} at temperatures below 273 K. The rate of crystallization of water in beef,¹¹ gluten,¹² and soybean constituents¹⁴ changed during cooling, as did the rate of melting of the thus formed ice during heating. The observations were described by a set of phenomenological equations for the aqueous solution ↔ ice phase equilibrium and the kinetics of the phase transformations.^{11,12}

Here we report a study which shows that the phenomenology of the water ↔ ice equilibrium in hydrated, pure proteins is qualitatively similar to that observed in the complex and inhomogeneous mixtures of native proteins and other materials.^{11,12,14} The same formalism that was used for describing the kinetics of crystallization of water in beef,¹¹ hydrated gluten,¹² and hydrated soybean proteins¹⁴ applies to hemoglobin and gliadin. The relative amount of water in equilibrium with ice in different proteins differs somewhat. Though much of this difference is due to the protein–water interactions, and not to the ionic and other impurities, the manner in which the thermodynamic equilibrium exists remains the same.

Experimental Methods

A 2.5 g sample of gliadin, which had been extracted from wheat flour, was provided to us by Drs. A. Buleon, Y. Popineau, and H. Bizot of Laboratoire de Physicochimie des Macromolécules of INRA, Nantes, France. As analyzed by them, the sample contained 6.97 wt % water, and on the basis of N 5.7, 88.7 wt % gliadins. The remaining 4.3 wt % substances were not characterized. They are likely to be carbohydrates and/or lipids. The sample provided by them contained a mixture of various gliadins and was studied without further purification. The sample treatment after preparation ensured that it contained little if any ionic salts. Hemoglobin (No. H 7379; source, human blood) was purchased from Sigma Chemical Co. (St. Louis, MO) and was used as such.

[⊗] Abstract published in *Advance ACS Abstracts*, July 1, 1997.

Hemoglobin and gliadin were hydrated by keeping small amounts of the samples in aluminum pans above the surface of water inside a sealed glass container at 298 K, as was done in the study of animal proteins.^{5–8} The amount of water in the hydrated polymer was determined by weighing the dry and the hydrated samples.

A differential scanning calorimeter (Model DSC 4 from Perkin-Elmer Corp.) with a TADS computer-assisted data acquisition system was used. The data acquisition software was written by one of us (G. Sartor), who had used it for earlier studies.^{4,5,16} The instrument was calibrated with 1-octanol and distilled water. Al-pans were used to contain the sample with an Al lid to cover it. Helium was used as a purge gas. During the DSC scan with a sample, a baseline recorded with empty aluminum pans was subtracted to remove the effects from the difference between the total thermal capacity of the instrument's sample holders and the Al pan on the sample side and the corresponding value on the reference side. For the heating rate of 30 K/min, the thermal lag of the instrument was 2.1 K. The DSC scans shown in all the figures here are corrected for the thermal lag.

The sample kept in the instrument was cooled either at the highest rate, which was found to be ≈ 150 K/min on calibration,⁴ or at 30 K/min, as noted in the text. The rate of heating for all DSC scans was 30 K/min. A total of 15–22 mg of the sample was used. The DSC output divided by the sample's mass remained the same for samples of different mass. This showed that the effect of the sample's mass on the measured values was negligible, if any.

Results

Earlier studies had shown that ice and aqueous solution coexist in hydrated beef¹¹ and hydrated gluten¹² to temperatures as low as 255 K. To examine whether the same occurs here, water-containing samples of hemoglobin and gliadin (both with 1 g of water/g of dry protein) were cooled from 298 to 170 K at 150 K/min and then heated at 30 K/min from 170 K to a certain temperature, T_a , chosen in the 263–274 K range, kept isothermally at T_a until a thermodynamic equilibrium, as detected by a constant isothermal DSC signal for 2 min, was established. The sample was then cooled at 30 K/min from T_a to 170 K, and the DSC scan was obtained during *cooling*. The scans for the hydrated gliadin are shown in Figure 1 and those for hydrated hemoglobin in Figure 2. The values chosen for T_a of hydrated gliadin were 274 K (curve 1) and 273 K (curve 2), 272 K (curve 3), 270 K (curve 4), 268 K (curve 5), 265 K (curve 6), and 263 K (curve 7) in Figure 1, and T_a for hydrated hemoglobin were 273 K (curve 1), 272 K (curve 2), 270 K (curve 3), and 268 K (curve 4) in Figure 2.

The area enclosed by a DSC scan in Figures 1 and 2 is a measure of the heat evolved during crystallization and other enthalpy and entropy changes due to a change in the number of configurational states of the biopolymer itself when water in it has crystallized. The DSC scans in Figures 1 and 2 show that, after annealing at each of the temperatures chosen as T_a in the 260–273 K range, a considerable amount of heat is still evolved on cooling the hydrated proteins and that the amount of this heat decreases with decrease in T_a . This means that, at temperatures below 273 K, ice coexists with water, or the aqueous solution, and with the proteins and other constituents of hemoglobin and gliadin. This coexistence at such high temperatures in the 260–273 K range, where the molecular diffusion time in pure water, as determined from dielectric measurements, is on the order of nanoseconds, indicates two thermodynamic aspects: (i) the free energy of ice and the liquid

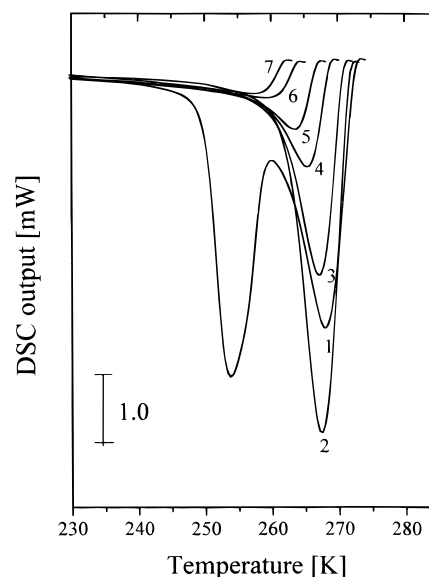


Figure 1. Plots showing the effects of high-temperature annealing on the DSC features of gliadin containing water in the ratio 1:1 (w/w). For the scans shown as curves 1–7, the sample was cooled from 298 to 170 K at 150 K/min and then heated at 30 K/min from 170 K to a different chosen temperature in the 263–274 K range, annealed for 2 min at that temperature, and thereafter scanned during *cooling* at 30 K/min from that temperature to 170 K. The annealing temperatures are 274 K (curve 1), 273 K (curve 2), 272 K (curve 3), 270 K (curve 4), 268 K (curve 5), 265 K (curve 6), and 263 K (curve 7).

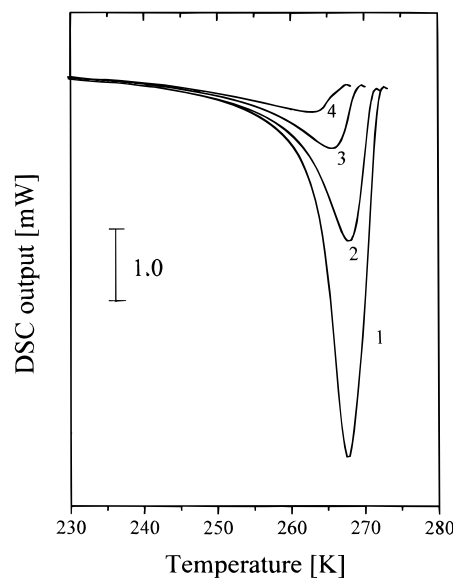


Figure 2. Plots showing the effects of high-temperature annealing on the DSC features of hemoglobin containing water in the ratio 1:1 (w/w). The scans, shown as curves 1–4, were obtained after heating the sample from 223 K to different chosen temperatures at 150 K/min, annealing for 5 min at that temperature, and thereafter scanning during cooling from that temperature to 223 K at 30 K/min. The annealing temperatures are 273 K for curve 1, 272 K for curve 2, 270 K for curve 3, and 268 K for curve 4.

phase, which is likely to be a freeze-concentrated solution in the case of hydrated, ionic salts, and impurity-containing proteins, is the same at these temperatures, and (ii) the amount of ice formed from the liquid is not determined entirely by the rate of (irreversible) crystallization during which impurities, e.g., ions and other organic substances, become segregated at the grain junctions of polycrystalline ice.

Before concluding that ice and water coexist at a thermodynamic equilibrium, it was necessary to determine, as before,^{11,12} whether the DSC scans of a sample cooled from a certain T_a

would be independent of the thermal treatment to which the sample had been subjected on thermal cycling in the range 260–273 K and whether the enthalpy released on its crystallization during cooling from T_a to 170 K would be independent of the thermal history of the sample. This was also necessary for ascertaining whether or not the sample had reached a thermodynamic equilibrium after 2 min annealing at T_a . For this purpose, samples of both hydrated gliadin and hemoglobin were cooled separately from 298 to 170 K at ≈ 150 K/min, heated to 268 K in the first set of our experiments, annealed at 268 K until a thermal equilibrium was attained, as observed by measuring the isothermal heat released, and then scanned to 170 K during cooling at 30 K/min. In the second set of experiments, the same sample was heated instead to 271 K, annealed at 271 K until it reached thermal equilibrium, and cooled to 268 K and again allowed to reach thermal equilibrium in 2 min. In several cases, 5 min was allowed for the equilibrium as in ref 11. It was thereafter scanned during cooling from 268 to 170 K at 30 K/min. In the third set, samples of hydrated gliadin and hemoglobin were thermally cycled between 170 and 272 K such that their thermal histories differed and brought to either 268 or 263 K. The samples were scanned during cooling from this temperature to 170 K at 30 K/min. The scans obtained from the first, second, and third sets of experiments were in reasonable agreement. The finding that a sample brought to T_a from a higher temperature, or a lower temperature, with or without thermal cycling, gave the same results indicates that equilibrium was reached in 2 min at T_a . Studies of isothermal DSC scans with time at temperatures as low as 250 K also showed that the exothermic signal became constant in less than 30 s. It is conceivable that grain growth of ice continued for a period longer than 30 s, but the heat evolved in the process is expected to be extremely small and is associated with the decrease in the surface energy, not the phase transformation. This also showed that the rate of cooling for the DSC scan was slow enough and the kinetics of crystallization fast enough to allow freezing of water. The areas above the exotherm obtained on cooling differed somewhat in each set of experiments by no more than 7%, and the exothermic minimum remained at the same temperature within 0.5 K. The former is attributable to the loss of water during the annealing procedure in these water-rich proteins or else to the variation in the amount of water that does not crystallize. Since the heat evolved on cooling from 268 to 170 K is equivalent to the total enthalpy of crystallization and any other changes, when the aqueous solution remains in equilibrium with ice, a change in this heat, as determined from the area circumscribed by the cooling scan, also indicates that the various contributions to enthalpy at 268 K depend on the thermal history of the sample.

Sartor and Mayer¹⁰ have observed a related effect in samples of 0.43 and 0.58 g of water/g of methemoglobin, but by measuring the melting endotherm after annealing the sample for different periods at 258 K to allow recrystallization of water in the samples. They found¹⁰ that the position of the melting endotherm as well its area changed as the fraction of recrystallized water changed on annealing the sample for different periods at 258 K and attributed this effect to the increase in the size of ice crystals. Doster et al.¹⁷ had discussed somewhat similar observations, but in terms of the depression of the melting point of ice in a myoglobin solution in terms of the Flory–Huggins model for polymer melting. It may be noted that although ionic concentrations in animal proteins may be large and may affect the freezing point of water by freeze concentration of the solutions on cooling below 273 K, such impurities are largely absent from gliadin studied here and in

gluten, studied earlier.¹² Such pronounced effects are not expected for these two proteins.

Curve 1 of Figure 1 shows a double crystallization peak for hydrated gliadin, and the reason for its appearance needs to be discussed. This DSC scan was obtained for the sample that had been thermally cycled (annealed, cooled, heated, and annealed) in the 260–272 K range and finally heated to 274 K, kept for 2 min, and then cooled at 30 K/min. This seems rather unusual, but Broto et al.¹⁹ have observed a similar effect in water–oil emulsions, where the water droplets were on the average 0.5 μm in diameter. The two crystallization exotherms vanished on keeping the water–oil emulsions for a few hours at 298 K. Here also fresh samples of gliadin did not show this effect. The reasons for the effect do not seem to be understood in detail, but they do show that redistribution of water occurs slowly even at 298 K in the water–oil emulsions¹⁹ and at 274 K in hydrated gliadin.

Discussion

Coexistence of Water and Ice in Proteins. The results given above demonstrate that there is no single thermodynamic freezing or crystallization temperature of the state of water in gliadin and hemoglobin. Rather, this thermodynamic freezing occurs over a broad temperature range, 273–233 K. Because most proteins contain organic and inorganic substances, it may seem that on cooling below 273 K water in them becomes freeze-concentrated as more and more ice forms. This depresses the freezing point of the remaining water in the freeze-concentrated solution further, as discussed by Doster et al.¹⁷ in a study of myoglobin and by Pruppacher and Klett¹⁸ as a general occurrence in nature. This is not likely to occur in the case of gliadin, as its purification procedure had already removed almost all of the NaCl and inorganic solutes from it. Thus, even though it contains a much lower concentration of ions than hemoglobin, it shows the coexistence of water and ice in its structure over as broad a temperature range as, and in a manner remarkably similar to, the hydrated hemoglobin in this study and beef,¹¹ soybean,¹⁴ and gluten¹² proteins containing water and a large variety of ionic and organic components in earlier studies. (A more recent, unpublished, study of water confined to the pores of poly(2-hydroxyethyl methacrylate), containing no impurities has shown a qualitatively similar behavior.) Hence, it seems that the coexistence of ice and water in proteins may not be entirely a consequence of the depression of the freezing point of water as impurities in it become progressively more freeze-concentrated.

The second reason may be that, in the microcrystalline ice formed, a large number of grain boundaries and grain junctions exist and that these grain junctions contain water in thermodynamic equilibrium with ice at temperatures substantially below 273 K. The latter occurrence is caused by a decrease in the free energy due to the curvature of the solid–liquid interface, as discussed and formulated earlier^{20,21} and observed for pure water inside the grain junctions of pure ice.²¹ This may contribute to some broadness of the temperature range of the water–ice coexistence in the proteins, but its magnitude is not expected to be as large as is observed here.

A third reason may be that water is confined to pores of varying size in the proteins, in the same manner as it is seen to be confined to the pores of poly(2-hydroxyethyl methacrylate), and that the nucleation followed by crystallization to ice does not as readily occur in smaller pores as in larger pores or that water in smaller pores supercools more readily than in the larger pores. This would be the case when the pores are disconnected from each other, so that the water–ice interface does not form

in any region connecting the pores. The melting point of a crystalline solid in a pore is already known to be lower the smaller the pore size, but it occurs only when the wall of the pore confining the solid is rigid and there is no interaction between the molecules forming the wall and the liquid confined by it, as implicit in the Gibbs–Thomson equation. (For a detailed discussion of the subject, a monograph, in ref 22, may be consulted.)

Inside a porous material, both liquid and solid can exist, when confined to different pores in the same material (smaller pores containing the liquid and the larger ones the solid), i.e., without an equilibrium that requires the Gibbs free energy of the solid in contact with liquid to be the same. Such studies have been made in Vycor or other types of porous glasses^{23,24} and porous minerals in nature and in carbon,²⁵ and a technique for porosimetry is based on measurements of the melting or freezing point of liquids in porous solids.²⁶ But proteins contain no pores with rigid walls and a well-defined geometry, and their OH and NH groups and N and O atoms interact with water through H-bonds. This would mean that none of the three factors mentioned above cause the water and ice to coexist over a broad temperature range and that the explanation may lie in the similarity between the nature of the H-bonds and other interactions in hydrated proteins.

An analysis of the exothermic features in the DSC scans of Figures 1 and 2 in terms of the water ↔ ice equilibrium is useful for understanding the H-bond interaction of proteins with water. Because of its purity, freeze concentration is not likely to occur in hydrated gliadin, and so the composition of the reactants (water–gliadin) and products (ice–gliadin) in it remained unaltered on changing the temperature. If freeze concentration also does not occur significantly on cooling hydrated hemoglobin below 273 K, an equilibrium constant, K_p , at a certain T_a , as defined below, may be calculated from the DSC scans in Figures 1 and 2.

$$K_p(T_a) = \frac{x_{\text{ice}}(T_a)}{x_{\text{liq}}(T_a)} = \frac{x_{\text{ice}}(T_a)}{1 - x_{\text{ice}}(T_a)} \quad (1)$$

where $x_{\text{ice}}(T_a)$ and $x_{\text{liq}}(T_a)$ are the fractional amounts of ice and liquid water, respectively, coexisting at T_a . The two coexist at other temperatures, when the rate of heating is low enough to allow a thermodynamic equilibrium to establish at each temperature during the cooling of the hydrated protein, but they are measured only at T_a here.

To determine x_{ice} at T_a , the DSC scans in Figures 1 and 2 may be used to obtain the ratio of the total heat evolved on cooling from T_a to the total heat evolved on cooling from 274 K or above to a low enough temperature, 230 K, where the phase transformation is almost complete or the amount of unfreezable water (in the well-known, traditional terminology²⁷) is sufficiently small to be ignored. From extrapolation of the (endothermic) heat of melting data of frozen beef containing different amounts of water, it was observed (Figure 10 in ref 11) that 0.011 mol, or 0.2 g, of water, per gram of dry beef protein does not freeze on cooling to 230 K. This extrapolation is based on the assumption that the heat absorbed on melting involves only the enthalpy of melting of ice and that none of the other eight effects summarized in eq 11 given in a later section here are significant in the melting temperature range. So, there seems to be an uncertainty in determining the amount of unfreezable water by calorimetry and the temperature limit up to which it remains unfrozen on cooling. Here it may also be recalled that crystallization requires aggregation of molecules as a result of their mutual diffusion, and that occurs when the

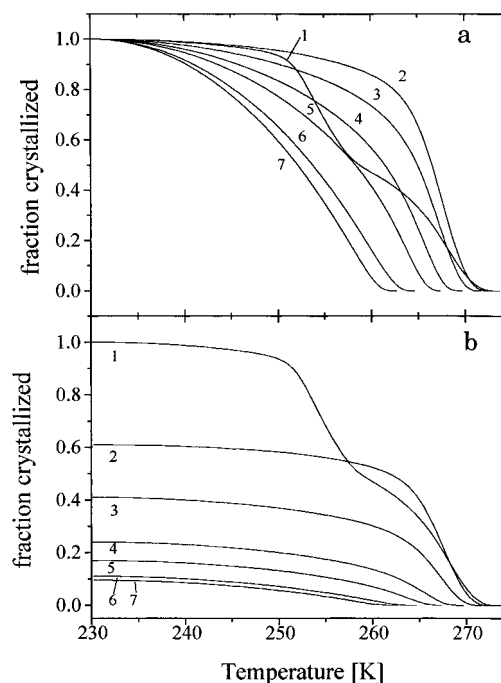


Figure 3. (a) Plots of the mole fraction of ice formed with respect to the total amount of ice formed on cooling gliadin containing water 1:1 (w/w), after annealing for 5 min at the temperatures as given in Figure 1. (b) Plots of mole fraction of ice formed on cooling the sample after annealing for 5 min at 273 K with respect to the total amount of ice formed on cooling from 273 K or above. The numbers next to the curves refer to the annealing conditions as given in Figure 1.

energy of their interaction with each other is lower than the energy of their interaction with the segments of the protein molecules. So, although a reason for the uncrystallizability of water in a protein may be given in general terms, it is not readily given quantitatively in energetic and kinetic terms.

The above-mentioned issues notwithstanding, the fractional amount of water crystallized on cooling from T_a to 230 K, or that of the ice formed, is given by

$$x_{\text{crystald}}(T) = \frac{\frac{1}{q} \int_{T_a}^T \left(\frac{\partial H}{\partial t} \right)_q dT}{\frac{1}{q} \int_{274K}^{230K} \left(\frac{\partial H}{\partial t} \right)_q dT} \quad (2)$$

where $\partial H/\partial t$ is the heat released per unit time (t in seconds) in the DSC measurements. The numerator in eq 2 is proportional to the amount of water that crystallized on cooling from T_a to T , after thermodynamic equilibrium is established at T_a , and the denominator is proportional to the total amount of the liquid water in the protein that crystallized on cooling from 274 K. The fraction that crystallized on cooling, x_{crystald} , is plotted against the temperature in Figure 3b for hydrated gliadin and in Figure 4b for hydrated hemoglobin. Each curve in these figures corresponds to a single T_a and was obtained from one DSC scan from among the ones shown in Figures 1 and 2, and they are labeled accordingly. In these plots, x_{crystald} for $T = 230$ K in eq 2 for hydrated gliadin and $T = 240$ K for hemoglobin represent the fractional amount of ice that formed on cooling from T_a . Therefore,

$$x_{\text{ice}}(T_a) = 1 - x_{\text{crystald}}(230 \text{ or } 240 \text{ K}) \quad (3)$$

is the amount of ice that coexisted with water at thermodynamic equilibrium at T_a . It should be stressed that this calculation is based on the assumption that the nature of interactions does not change on cooling, so that the heat released at all

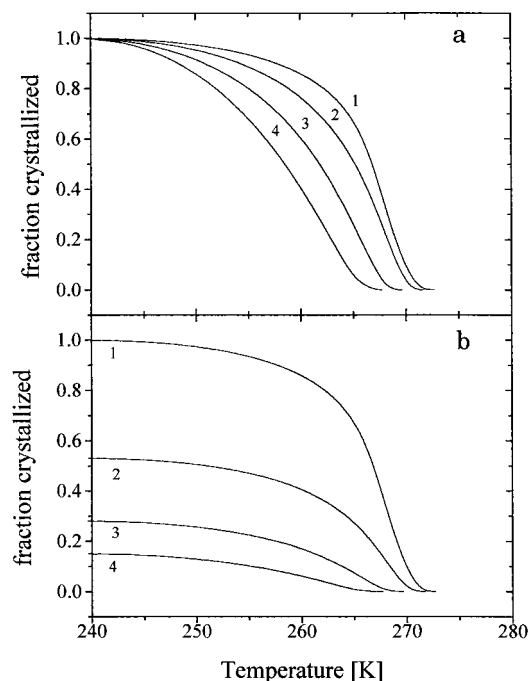


Figure 4. Frames a and b contain plots that correspond to the same quantities as in Figure 3, but here these quantities are for hemoglobin. The numbers next to the curves refer to the annealing conditions as given in Figure 2.

temperatures remains proportional to the amount of water crystallized to ice.

According to the Gibbs–Helmholtz equation,²⁸ the enthalpy of phase transformation, ΔH° , is related to the change in free energy, ΔG° , by

$$\left(\frac{\partial(\Delta G^\circ/T)}{\partial T}\right)_p = -\frac{\Delta H^\circ}{T^2} \quad (4)$$

where substituting by $\Delta G^\circ = -RT \ln K_p$ yields the van't Hoff equation

$$\left(\frac{\partial \ln K_p}{\partial T}\right)_p = \frac{\Delta H^\circ}{RT^2} \quad \text{or} \quad \left(\frac{\partial \ln K_p}{\partial (1/T)}\right)_p = -\frac{\Delta H^\circ}{R} \quad (5)$$

It is expected that ΔH° calculated from K_p according to eq 5 should be the same as ΔH_m ($=6.01$ kJ/mol), the enthalpy of freezing of pure water at 273.16 K. Hence, any deviation from eq 5, and the difference between ΔH° and ΔH_m , may be seen as a reflection of a change in the composition of the two states with changing temperature. From eq 3 and the values of $x_{\text{crystalld}}$ at the lowest temperature, as seen in Figures 3b and 4b, $x_{\text{ice}}(T_a)$ in equilibrium with water in hydrated gliadin at the annealing temperature, T_a , is 0.39 at 273 K, 0.59 at 272 K, 0.76 at 270 K, 0.83 at 268 K, 0.89 at 265 K, and 0.905 at 263 K. Curve 1 in Figure 5 shows the plot of x_{ice} against T_a . Thus, K_p was calculated from eq 2 using the values of x_{ice} in equilibrium with water and was plotted logarithmically against $1/T$. The plot was a curved line whose slope decreased on increasing the temperature, and its slope gave $\Delta H^\circ \gg \Delta H_m$ at all temperatures, as was found in the studies of beef¹¹ and gluten.¹² This seems to be evidence that the enthalpy of water itself is altered by the protein's strong interactions, or else other effects contribute to the thermodynamics of water \leftrightarrow ice equilibrium in gliadin and hemoglobin.

Kinetics of Crystallization from the Liquid Phase. The kinetics of crystallization of ice from the water in the hydrated gliadin on cooling from a temperature $T_a < 273$ K to 170 K at

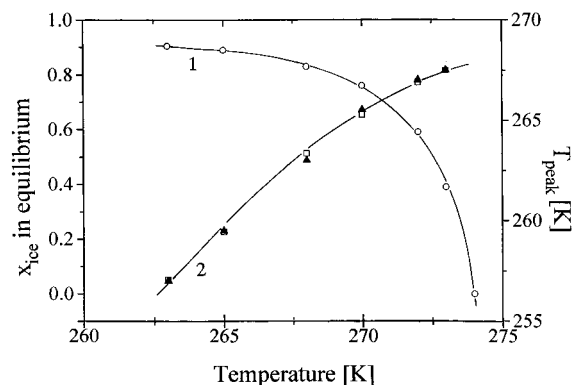


Figure 5. Curve 1 is a plot of the fractional amount of ice (open circles) that is in equilibrium with water in hydrated gliadin at the annealing temperatures as given for curves 1–7 in Figure 1. Curve 2 is a plot of the temperature of the crystallization peak (scale on right) against the annealing temperature. Squares are the experimental values from Figure 1, and the filled triangles are the calculated values.

a certain rate, q , may be discussed quantitatively in terms of three formalisms:^{11,12} two for the nucleation and grain-growth processes and one for only the grain-growth process. The first is in terms of an empirical equation,^{29–31} according to which the fraction crystallized at time t , $f_x(t)$, is given by

$$f_x(t) = x/x_0 = 1 - \exp(-kt^n) \quad (6)$$

where x is the amount crystallized, x_0 is the initial amount of the uncrystallized material at $t = 0$, k is the temperature-dependent crystallization rate which includes both crystal nucleation and growth, and n varies between 0.5 and 4, depending upon the nucleation mechanism and growth morphology. For a fixed temperature, k may depend upon time, as Hage et al.³² have observed, or may not, as is assumed in most studies of crystallization kinetics. Equation 6 applies to a process when there is no phase equilibrium between the crystallized and uncrystallized states and the crystallization process is irreversible, as its occurrence brings a thermodynamically metastable state to a state of lower energy.

The second phenomenological description, developed specifically for proteins,^{11,12} is in terms of the increasing fraction of ice with decreasing temperature, according to the variation of the constant for the water \leftrightarrow ice equilibrium and of the limits imposed by the cooling rate on this fraction. For using both descriptions, we need to obtain $f_x(T)$, the fraction of ice formed at a temperature, T , on cooling the sample at a rate, q ($=\partial T/\partial t$), from the temperature at which it was annealed, T_a , to 240 K. The partial area of the exotherm at a temperature, T , is equivalent to the heat evolved on crystallization during cooling to that temperature, and so

$$f_x(t) = \frac{\frac{1}{q} \int_{T_a}^T \left(\frac{\partial H}{\partial t}\right)_q dT}{\frac{1}{q} \int_{T_a}^{240\text{K}} \left(\frac{\partial H}{\partial t}\right)_q dT} \quad (7)$$

where the integral in the denominator is equivalent to the total amount of ice formed on cooling, from T_a , or the total amount of water present at T_a . (Note that this equation is valid generally when the molar heat of crystallization does not depend upon the temperature and, as in the case here, also does not change on freeze concentration of the liquid.) The value of $f_x(T)$, which is equal to the amount of water crystallized with respect to the amount of water in hydrated gliadin and hemoglobin present at T_a after thermal equilibrium had been established at T_a , was calculated from eq 7 and the data in Figure 1. It is plotted

against the temperature in the upper part of Figure 3a, where each curve is for a sample of different T_a . The corresponding plots for hydrated hemoglobin are shown in Figure 4a. The shape of these plots is an inverted sigmoid, which changes with change in T_a . This change is attributable to the change in the rate of crystallization on changing T_a as well as T . The double-sigmoid shape of curve 1 is a reflection of two exothermic peaks, as discussed earlier here and observed also for water–oil emulsions.¹⁹

Ice grains of course already exist at all T_a 's at or below 273 K. Confined to connected pores, these grains are small and may grow on cooling. So, it seemed necessary to consider simulating the DSC scans by using empirical equations for the kinetics of the grain-growth process.³³ But this consideration also did not lead to a satisfactory simulation because the DSC scans for the grain-growth process are skewed at the high-temperature side of the exothermic peak,³³ which is the opposite of the observation in Figures 3a and 4a and in Figures 1 and 2 where the DSC scans are skewed at the low-temperature side of the exothermic peak.

The second procedure for the analysis is in terms of crystallization kinetics where a temperature-dependent crystallization rate is considered^{11,12} within the bounds of equilibrium thermodynamics; i.e., the equilibrium constant changes with temperature. At this equilibrium, the liquid water, not the hydrated protein, is an aqueous solution containing dissolved impurities. This liquid is in equilibrium with the hydrated protein in which the H_2O molecules are H-bonded to the protein's N- and O-containing groups and to those H_2O molecules that are on the surface of the crystallized ice as well as the ice itself. We postulate that the rate kinetics of this equilibrium is determined by the partial reorientation of the protein molecule, so that the transformation, (hydrated) protein + water \leftrightarrow (hydrated) protein + ice, involves two rates, k_1 in the forward direction and k_2 in the reverse direction. These two are related to

$$X(T) = \frac{k_1(T)}{k_2(T)}; \quad k_2(T) = \frac{k_1(T)}{X(T)} \quad (8)$$

and

$$X(T) = \frac{x_{ice}(T)}{x_{liq}(T)} = \frac{f_x(T)}{1 - f_x(T)} \quad (9)$$

where $X(T)$ is equivalent to K_p , for which a comparison against the Gibbs–Helmholtz equation has already shown a strong H-bond interaction of water molecules with the proteins. $X(T)$ is known from experiments for six temperatures, which are the annealing temperatures in Figures 1–4. $k_1(T)$ is written by the Arrhenius equation,

$$k_1(T) = k_0 \exp(-E^*/RT) \quad (10)$$

where k_0 is the preexponential factor and E^* is the activation energy. The solution for the equations for the rate constants k_1 and k_2 in terms of the concentration of the product is given in earlier papers,^{11,12} as has the formalism and the procedure for simulation that is to be used here. The values of k_0 and E^* of eq 9 must be such that they are applicable for simulations of all DSC scans except curve 1, as shown in Figure 1, and because of this, their arbitrariness is less serious. The ΔC_p used varied for different scans and decreased with increase in T_a . For the simulation of the DSC scan of hydrated gliadin, $k_0 = 5.79 \times 10^4 \text{ s}^{-1}$, $E^* = 30.05 \text{ kJ/mol}$, and $\Delta C_p = 0.0, 0.60, 0.45, 0.50, 0.60$, and $0.60 \text{ J/K}^{-1} \text{ g}^{-1}$ for $T_a = 273, 272, 270, 268, 265$, and

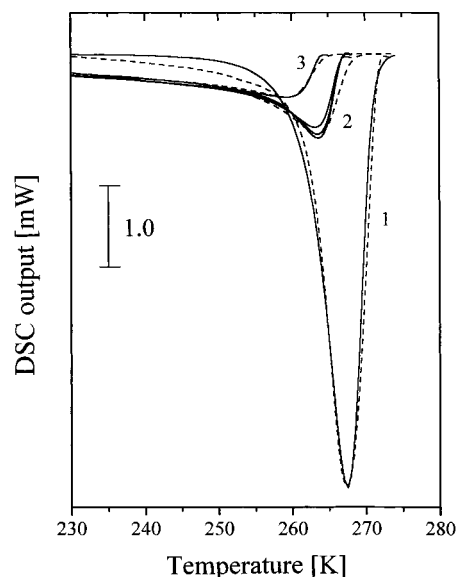


Figure 6. Typical plots showing a comparison of the experimentally obtained DSC curves (continuous line) for a 1:1 (w/w) water–gliadin mixture and those calculated (dashed line) with the parameters given in the text.

263 K, respectively, were used. The corresponding values for gluten¹² are $k_0 = 5.50 \times 10^4 \text{ s}^{-1}$, $E^* = 31.2 \text{ kJ/mol}$, for soybean¹⁴ are $k_0 = 5.05 \times 10^4 \text{ s}^{-1}$, $E^* = 29.4 \text{ kJ/mol}$, and for beef¹¹ are $k_0 = 5.02 \times 10^4 \text{ s}^{-1}$, $E^* = 29.75 \text{ kJ/mol}$. These values seem to be very similar for the three proteins, despite the difference in their structure and the amount and type of impurities present in them. Furthermore, the magnitude of E^* , which is twice the magnitude of the H-bond energy, indicates that crystallization involves breaking of at most two H-bonds. It is not known whether the rate process is of first order or higher.

A comparison between the curves simulated (broken line) from the parameters given above and the procedure described before and the measured DSC scans (continuous line) for $T_a = 273, 265$, and 268 K are shown as sets 1, 2, and 3, respectively, in Figure 6. From the agreement observed between the simulated and measured DSC scans, it is evident that the crystallization kinetics at $T_a < 273 \text{ K}$ is satisfactorily described by eqs 6–10. For a further comparison of the simulation against the measured data, the temperatures of the calculated and measured exothermic minima are plotted against T_a as curve 2 in Figure 5. The agreement between the calculated (squares) and measured (filled triangles) values seems satisfactory in all experiments. This clearly demonstrates that the theoretical considerations of the water–ice phase transformation given here have merit and may be further examined by experiments on other proteins and complex H-bonded molecules.

Comparison between the Water–Ice Equilibrium in Different Proteins. The fractional amount of water in equilibrium with ice in gliadin, hemoglobin, beef,⁹ gluten,¹⁰ and soybean¹² proteins, which is plotted against the temperature in Figure 7, shows that the variations of water fraction in the five proteins are similar, although their amounts differ by as much as a factor of 2 at certain temperatures. The difference between the amounts are important because the presence of water in a protein at subfreezing temperatures allows it to remain biologically active. As the data have been obtained from the measurements of the heat evolved during cooling, a thermodynamic interpretation of the source of this heat seems appropriate here.

The enthalpy and entropy changes during cooling of a hydrated protein or biopolymer represent an overall effect of

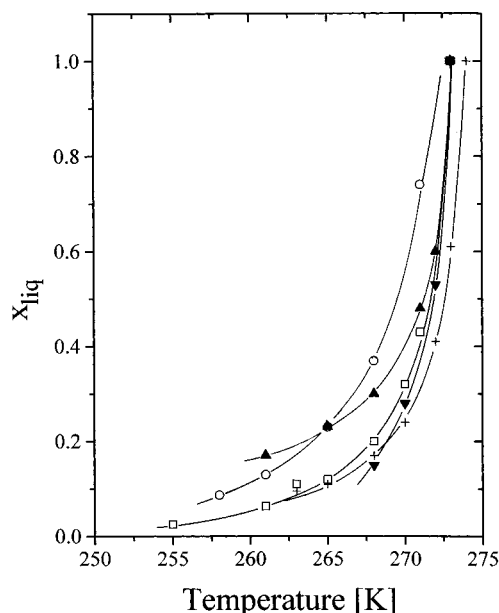


Figure 7. Mole fraction of liquid water present in the various proteins at different annealing temperatures is plotted against the annealing temperature. The notations are (▼) hemoglobin, (+) gliadin, (□) beef (ref 11), (○) soybean (ref 14), and (▲) gluten (ref 12).

several occurrences, namely, (i) the heat evolved on crystallization of water to ice, (ii) a change in the interfacial energy between the ice grains formed due to a change in the grain size, (iii) a change in the total number of H-bonds, (iv) the loss of configurational contribution to the enthalpy and entropy of the protein molecule when water crystallized and lost its ability to diffuse translationally, thereby reducing the configurational and conformational degrees of freedom of a protein molecule's segments, (v) the heat evolved on ion pair formation when the protein contains ions, (vi) the heat associated with the precipitation of ionic salts used as buffering agents, (vii) a reversible isomerization of the organic impurities in the protein, (viii) the heat associated with the precipitation or dissolution of any organic impurity, and (ix) the heat of solution of the precipitated inorganic and organic impurities in the remaining liquid water (also known as freeze-concentration)

$$\Delta H = [\Delta H_{\text{cryst}} + \Delta H_{\text{interf}}] + [\Delta H_{\text{H-bonds}} + \Delta H_{\text{conf}}] + [\Delta H_{\text{ion-pair}} + \Delta H_{\text{salt-pptn}}] + [\Delta H_{\text{isom}} + \Delta H_{\text{org-imp}}] + \Delta H_{\text{soln}} \quad (11)$$

where the nine terms on the right-hand side of eq 11 refer to effects i through ix, as described above. Among these, effect i is expected to be most prominent in all cases, and effects v–ix are expected to be absent from gliadin because of the absence of ionic impurities in it. The relative merits of these effects are yet to be critically examined in detail using different experimental techniques, but it may be stressed that the phenomenon reported here is mimicked by water-containing poly(2-hydroxyethyl methacrylate), a polymer used for soft contact lenses which is free from inorganic and organic impurities. This alone lends support to our premise that the freeze concentration of water only is not at the origin of the water–ice equilibrium in proteins.

ΔH_{cryst} itself decreases with the temperature,³⁴ and its value is likely to be the same for all the five proteins, particularly when they are water-rich. Among the remaining eight contributions to ΔH , as given in eq 11, $\Delta H_{\text{H-bonds}}$ and ΔH_{conf} are determined by the protein's structure, and the remainder of the terms are determined by the nature of the impurities, such as

buffering agents and organic substances present. Some of these terms, particularly, $\Delta H_{\text{salt-pptn}}$, $\Delta H_{\text{org-imp}}$, and ΔH_{soln} , are usually endothermic, which may partially reduce the exothermic effects. This entails the amount of water deduced from the calorimetric data being less than the actual value. Our studies in future will be aimed at investigating these effects in well-characterized aqueous solutions, although such effects are expected to be small in comparison with the ΔH_{cryst} of 334 J/g of water at 273.16 K. We conclude that the difference between the amounts of water in different proteins is a reflection of the difference between the contribution to the various ΔH terms listed in eq 11 and that the lowest value for water's fraction in hydrated gliadin seen in Figure 7 is likely to be due to the effects iii and iv. Nevertheless, a more critical examination of the nine effects mentioned above is needed by experiments using different techniques and well-characterized samples in which the magnitude of the different effects can be controlled.

Acknowledgment. G. Sartor is grateful to the Fonds zur Förderung der Wissenschaftlichen Forschung (FWF) of Austria for providing a Schrödinger scholarship. This research was partly supported by the Natural Sciences and Engineering Council of Canada.

References and Notes

- (1) Frauenfelder, H.; Parak, F.; Young, R. D. *Annu. Rev. Biophys. Biophys. Chem.* **1988**, *17*, 451.
- (2) Privalov, P. L. *Annu. Rev. Biophys. Biophys. Chem.* **1989**, *18*, 47.
- (3) See for example, chapters and references in: *Protein-Solvent Interaction*; Gregory, R. B., Ed.; Marcel Dekker: New York, 1994. See also references listed in: Green, J. L.; Fan, J.; Angell, C. A. *Ibid* **1994**, *98*, 13780, and further in ref 7.
- (4) Sartor, G.; Hallbrucker, A.; Hofer, K.; Mayer, E. *J. Phys. Chem.* **1992**, *96*, 5133. Glass liquid transition and crystallization of a vitreous, but freezable, water fraction in hydrated methemoglobin. In *Water Biomolecule Interactions, Conference Proceedings*; Palma, M. U., Palma-Vittorelli, M. B., Parak, F., Eds.; SIF: Bologna, p 143.
- (5) Sartor, G.; Mayer, E.; Johari, G. P. *Biophys. J.* **1994**, *66*, 249.
- (6) Sartor, G.; Hallbrucker, A.; Mayer, E. *Biophys. J.* **1995**, *69*, 2679.
- (7) Rudisser, S.; Hallbrucker, A.; Mayer, E. *J. Phys. Chem.* **1996**, *100*, 458.
- (8) Rudisser, S.; Hallbrucker, A.; Mayer, E.; Johari, G. P. *J. Phys. Chem. B* **1997**, *101*, 266.
- (9) Sartor, G.; Mayer, E.; Johari, G. P. *Biophys. J.* **1995**, *69*, 249.
- (10) Sartor, G.; Mayer, E. *Biophys. J.* **1994**, *67*, 1724.
- (11) Sartor, G.; Johari, G. P. *J. Phys. Chem.* **1996**, *100*, 10450. Its eqs 3 and 4 should be read as eqs 4 and 5 in this paper. The DSC output in the figures is in mW/mg.
- (12) Johari, G. P.; Sartor, G. *J. Chem. Soc., Faraday Trans.* **1996**, *92*, 4521. Its eqs 4 and 5 should be read as eqs 4 and 5 in this paper. The DSC output in the figures is in mW/mg.
- (13) Sartor, G.; Johari, G. P. *J. Phys. Chem.* **1996**, *100*, 19692. The DSC output in the figures is in mW/mg.
- (14) Johari, G. P.; Sartor, G. In *Proceedings of ISOPOW V Conference*; Taylor & Francis: London, in press. The DSC output in the figures is in mW/mg.
- (15) Hofer, K.; Mayer, E.; Johari, G. P. *J. Phys. Chem.* **1990**, *94*, 2689.
- (16) Sartor, G.; Mayer, E.; Johari, G. P. *J. Polym. Sci. B, Polym. Phys.* **1994**, *32*, 683.
- (17) Doster, W.; Bachleitner, A.; Dunau, R.; Hiebel, M.; Luscher, E. *Biophys. J.* **1986**, *50*, 213.
- (18) Pruppacher, H. R.; Klett, J. D. *Microphysics of Clouds and Precipitation*; D. Reidel: Dordrecht, 1980; pp 149–161.
- (19) Broto, F.; Clausse, D. *J. Phys. C* **1976**, *9*, 4521. See also: *J. Phys. Chem.* **1983**, *87*, 4030.
- (20) Johari, G. P.; Pascheto, W.; Jones, S. J. *J. Chem. Phys.* **1994**, *100*, 4548.
- (21) Salvetti, G.; Tombari, E.; Johari, G. P. *J. Chem. Phys.* **1995**, *102*, 4987.
- (22) Defay, R.; Prigogine, I.; Bellemans, A.; Everett, D. H. *Surface Tension and Adsorption*; Wiley: New York, 1966.
- (23) Jackson, C. L.; McKenna, G. B. *J. Chem. Phys.* **1990**, *93*, 9002.
- (24) Handa, Y. P.; Zakrzewski, M.; Fairbridge, C. *J. Phys. Chem.* **1992**, *96*, 8594.

- (25) Sartor, G.; Johari, G. P. Unpublished study.
- (26) Quinson, J. F.; Brun, M. In *Characterization of Porous Solids*; Unger, K. K., Rouquerol, J., Sing, K. S. W., Kral, K., Eds.; Elsevier: Amsterdam, 1988; p 307.
- (27) Kuntz, I. D.; Simatos, D. In *Water Relations of Foods*; Duckworth, R. B., Ed.; Academic Press: New York, 1975; p 187.
- (28) Atkins, P. W. *Physical Chemistry*, 3rd ed.; Oxford University Press: London, 1986; p 702.
- (29) Johnson, W. A.; Mehl, R. F. *Trans. AIME* **1939**, 416, 135.
- (30) Avrami, M. *J. Chem. Phys.* **1939**, 7, 1103; **1940**, 8, 212; **1941**, 9, 177.
- (31) Christian, J. W. *The Theory of Transformation in Metals and Alloys*, 2nd ed.; Pergamon Press: New York, 1975; pp 525–548.
- (32) Hage, W.; Hallbrucker, A.; Mayer, E.; Johari, G. P. *J. Chem. Phys.* **1995**, 103, 545.
- (33) Ram, S.; Johari, G. P. *Philos. Mag. B* **1990**, 61, 299.
- (34) Johari, G. P.; Fleissner, G.; Hallbrucker, A.; Mayer, E. *J. Phys. Chem.* **1994**, 98, 4719.